REPORT DOCUMENTATION PAGE

Form Approved OMB NO. 0704-0188

1. REPORT DATE (DD-MM-YYYY)	2. REPORT TYPE	3. DATES COVERED (From - To)
26-08-2009	Final Report	1-Aug-2006 - 31-Jul-2009

4. TITLE AND SUBTITLE
GALVANIC CORROSION IN SILICON MICROSYSTEMS: IMPACT ON MATERIAL PROPERTIES AND DEVICE PERFORMANCE

5a. CONTRACT NUMBER
W911NF-06-1-0342

5b. GRANT NUMBER

5c. PROGRAM ELEMENT NUMBER
611102

6. AUTHORS
Conrad R. Stoldt

5d. PROJECT NUMBER

5e. TASK NUMBER

5f. WORK UNIT NUMBER

7. PERFORMING ORGANIZATION NAMES AND ADDRESSES
University of Colorado - Boulder
Office of Contracts and Grants
Campus Box 572, 3100 Marine Street Rm 481
Boulder, CO 80309 -0572

8. PERFORMING ORGANIZATION REPORT NUMBER

9. SPONSORING/MONITORING AGENCY NAME(S) AND ADDRESS(ES)
U.S. Army Research Office
P.O. Box 12211
Research Triangle Park, NC 27709-2211

10. SPONSOR/MONITOR'S ACRONYM(S)
ARO

11. SPONSOR/MONITOR'S REPORT NUMBER(S)
49597-MS.1

12. DISTRIBUTION AVAILIBILITY STATEMENT
Approved for Public Release, Distribution Unlimited

13. SUPPLEMENTARY NOTES
The views, opinions and/or findings contained in this report are those of the author(s) and should not contrued as an official Department of the Army position, policy or decision, unless so designated by other documentation.

14. ABSTRACT
Many microsystems fabrication technologies currently employ a metallic overlayer, such as gold, in electrical contact with silicon (Si) structural layers. During postprocessing in hydrofluoric acid based solutions, a galvanic cell is created between the silicon and the metallic layer. As a consequence, autonomous corrosion (etching) of the silicon layer occurs forming nanoscale porosity at the thin film surface and grain boundaries. Over the past 24 months, our ARO sponsored work on microfabricated polycrystalline silicon (polySi) and single crystal Si (SCS)

15. SUBJECT TERMS
Corrosion, Silicon, MEMS, Finite Element Method

16. SECURITY CLASSIFICATION OF:			17. LIMITATION OF ABSTRACT	15. NUMBER OF PAGES	19a. NAME OF RESPONSIBLE PERSON
a. REPORT	b. ABSTRACT	c. THIS PAGE			Conrad Stoldt
U	U	U	SAR		19b. TELEPHONE NUMBER 303-492-7698

U.S. Army Research Office grant no. W911NF-06-1-0342
Progress Report for April – August 2009 and Overall Project Summary

GALVANIC CORROSION IN SILICON MICROSYSTEMS: FINITE ELEMENT SIMULATION TOOL DEVELOPMENT

Prof. Conrad R. Stoldt
Department of Mechanical Engineering, University of Colorado, Boulder, CO USA 80309-0427
Email: stoldt@colorado.edu; Phone: (303) 492-7698

Overview

Many microsystems fabrication technologies currently employ a metallic overlayer, such as gold, in electrical contact with silicon (Si) structural layers. During postprocessing in hydrofluoric acid based solutions, a galvanic cell is created between the silicon and the metallic layer. As a consequence, autonomous corrosion (etching) of the silicon layer occurs forming nanoscale porosity at the thin film surface and grain boundaries. Over the past 24 months, our ARO sponsored work on microfabricated polycrystalline silicon (polySi) and single crystal Si (SCS) shows that electrochemical corrosion can significantly degrade key operational characteristics including stiffness, strength, electrical resistance, and surface morphology. Following characterization and quantification of Si corrosion, we have developed a corrosion simulation tool for microsystems that can be used to predict property degradation including modulus and fracture strength. Designers can also use this model to identify corrosion susceptible device geometries, enabling subsequent design alteration to reduce corrosion or limit corrosion to non-critical areas of the device. The end goal of this research effort being the realization of unprecedented material properties and performance in Si based MEMS through rational design, testing, and simulation.

Micro-tensile tests

In our 2007 work, we utilized micromachined polySi and SCS tensile specimens to further elucidate the impact of electrochemical corrosion on microsystem performance and reliability [1,2]. Analysis of the corroded tensile specimens revealed a catastrophic reduction in tensile strength and apparent modulus of the structural Si. In both polySi and SCS samples, corrosion resulted in a thick corroded layer created via porous Si formation and/or generalized material removal depending on the etch chemistry and conditions employed. The nature and severity of corrosion damage are influenced by the surface wetting characteristics of the etch chemistry, the etch duration, and the thin film microstructure.

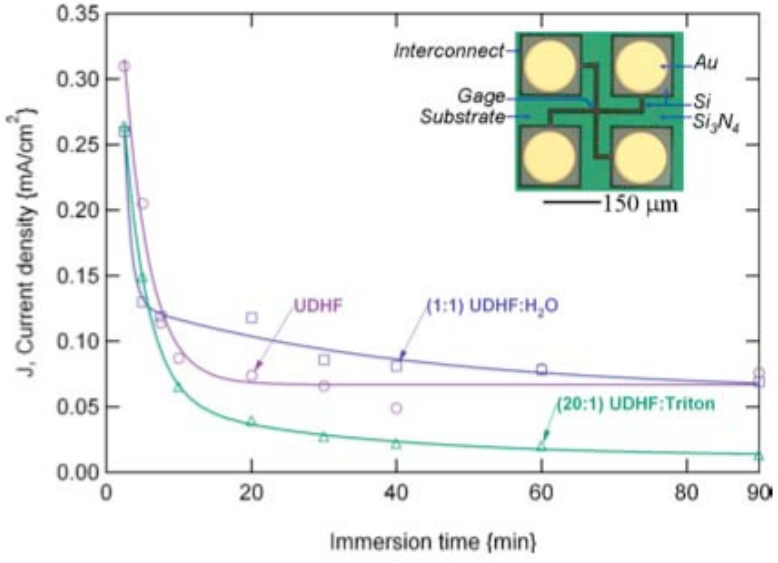

Figure 1: Corrosion rate determined using polySi resistive probes for three different etchant chemistries. An optical micrograph of the test structure is shown in the inset.

Electrochemical characterization

In 2008, we extended this work to the fundamental characterization of corrosion on thin film polySi and SCS surfaces [3]. Here, microscale Si resistive probe devices were designed and fabricated to relate the measured electrical resistance to material consumption after electrochemical etching. The resistive probe is a technique commonly used to monitor or predict corrosion in macroscopic systems such as in marine vessels, but has previously not been miniaturized for microscale corrosion diagnostics. The resistive probes consist of four-point "Van der Pauw" structures fabricated via the SOIMUMPs or polyMUMPs technologies. PolySi and SCS resistive probe devices were employed to connect etchant specific damage to the physio-chemical nature of the corrosion process. For example, the current density measured as a function of etchant immersion time is shown in Figure 1 for three different etch chemistries. The current density data, and the resulting calculated etch rates, were shown to be quantitatively similar to those measured using the microtensile specimens [2].

Recent Progress: Corrosion FEM development

In the last year, we have been developing a finite element simulation to model electrochemical corrosion in MEMS. The resistive probe structures described in the previous section of this report are used to predict current density and subsequent Si damage as a function of the surface area ratio (SAR) of Au relative to Si in HF electrolyte solutions [3]. Specifically, current density and subsequent damage is observed to increase as SAR is increased. To date, the corrosion of microsystems components has not been specifically analyzed using modeling techniques. To this end, the effect of three-dimensional (3-D) geometry as well as the proximity to the cathode to the anode remain unexplored. We believe that modeling may therefore provide a fundamental understanding, aiding to mitigate corrosion damage.

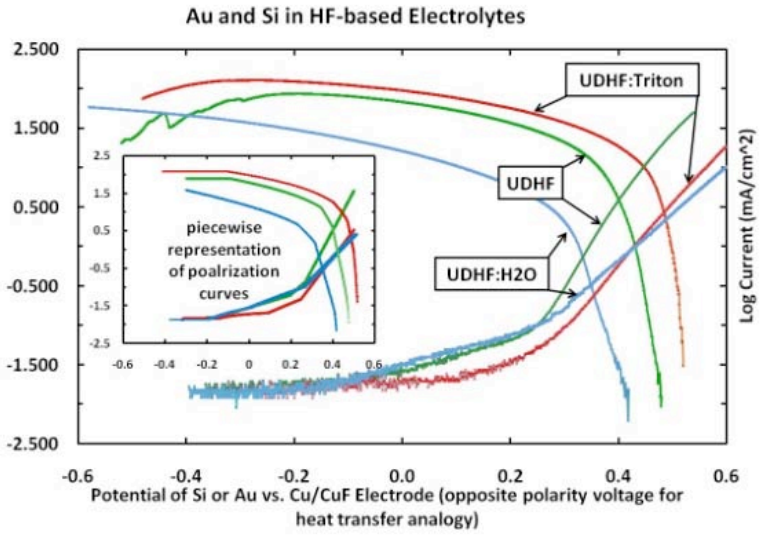

Figure 2: Empirical Tafel plots of Si/Au in the three HF electrolytes. The inset shows the curves represented by piecewise Tafel equations. It is noted that the sign convention of the plot has been reversed according to the heat transfer analogy.

The numerical modeling of electrochemistry and corrosion are typically based on the Boundary Element Method (BEM) or the Finite Element Method (FEM) [4]. FEM may include interfacial properties and transport through an electrolyte. Therefore FEM is the ideal tool to model a 3-D design where geometrical constraints may enhance or reduce corrosion [4-7]. FEM allows designers to predict the location of the greatest corrosion damage and defer damage to non-critical components or areas. The value of FEM includes: non-linear polarization curves may be incorporated in the simulation, the entire electrolyte body may be considered - revealing the potential distribution in the solution, complex 3-D geometry may be incorporated - where the geometry as well as boundary conditions may be modified as necessary [7].

The goals of this ARO finite element modeling initiative are to reveal the effects of geometry, SAR, and electrolyte composition on corrosion in microsystems using both physical inspection of resistive probe devices and FEM modeling. To identify the extent of corrosion (by investigating PS thickness as a function of distance from a Au cathode), focused ion beam (FIB) in conjunction with field emission scanning electron microscopy (FE-SEM) are used to image the cross section of the resistive probe structures. Analytical results from the literature as well as BEM simulation [8,9] of a simple cube structure of an anode and cathode are used to first calibrate and demonstrate proper functionality of the FEM model. Data recently obtained using four point resistive probe structures [3] is then compared to FEM results. The cross section and modeling results reveal that for the four point probe structures investigated, corrosion is uniform across the entire exposed Si surface. This result is significant in that corrosion reports on more tradition materials such as magnesium and steel in sodium chloride electrolyte reveal a gradient in corrosion magnitude that is greatest near the cathode [9]. The model also predicts the appropriate trend of increasing current density seen with SAR on the resistive probes [3].

In building the simulation program, we generated empirical polarization curves for polySi and SCS with Au in three HF electrolytes (shown in Figure 2), the results of which are linearized to obtain the Tafel coefficients that are referenced in the finite element model subroutine. To verify appropriate interaction between the electrodes and the electrolyte in the FEM analysis, the FEM solution was compared against a more basic geometry solved using the finite difference method (FDM) as in Ref. [8] and the BEM (BEASY, BEASY Software solution) as in Ref. [9]. For verification, the anode and cathode are represented as two separate cubes and the electrolyte is modeled as a cube of varying height (simulating varying the depth of electrolyte over the immersed anode and cathode. In the two verification analyses, a 2D representation is utilized such that the electrodes and electrolyte are of infinite in-plane thickness, however the FEM model must be created as a 3D structure i.e. finite size in all dimensions.

The results of a model of the potential in the electrolyte for unique electrolyte heights are shown in Figure 3. The results compare identically to those presented in Ref. [9]. Additionally, the potential at varying cross sections within the electrolyte corresponds to those results presented by Doig and Flewitt [8]. These results ensure that the 3D FEM model is correctly calibrated to reproduce the 2D FDM and BEM solutions.

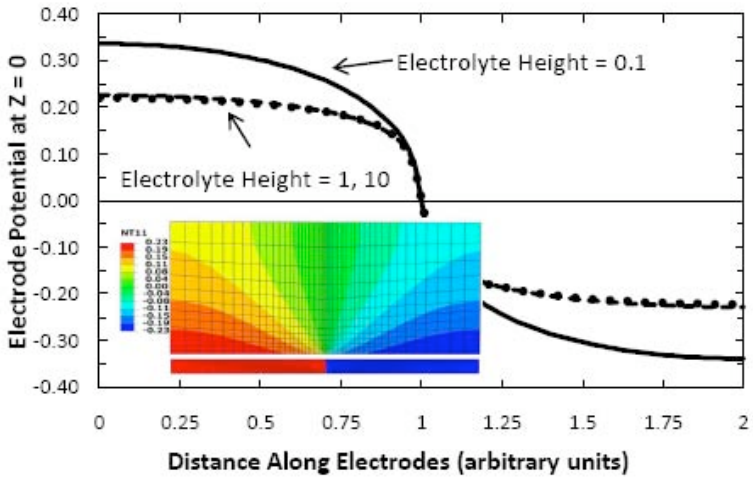

Figure 3: Validation of FEM model by comparison against FDM and BEM using a simply geometry: (inset) The computed electric field potential distribution (shown with the mesh included) from parts). The plots shows the potential in the electrolyte along the surface of the anode and cathode for three different electrode separation distances.

The results shown in Figure 3 also give insight into the effect of electrolyte depth (in other words, the height of the electrolyte in the FEM model) on potential and current density, an effect that must be evaluated numerically rather than analytically [8,9]. As the height decreases, the isopotential field lines are normal to the electrode surface. As the

height is increased, the field lines become more parallel to the electrode surface [8]. The field distribution depicted in Figure 3 importantly identifies that to accurately model an electrochemical interaction in which the electrolyte depth is nearly infinite with respect to the dimensions of an immersed electrode, the electrolyte needs to be modeled as a body with a height on the order of the dimensions of the electrodes.

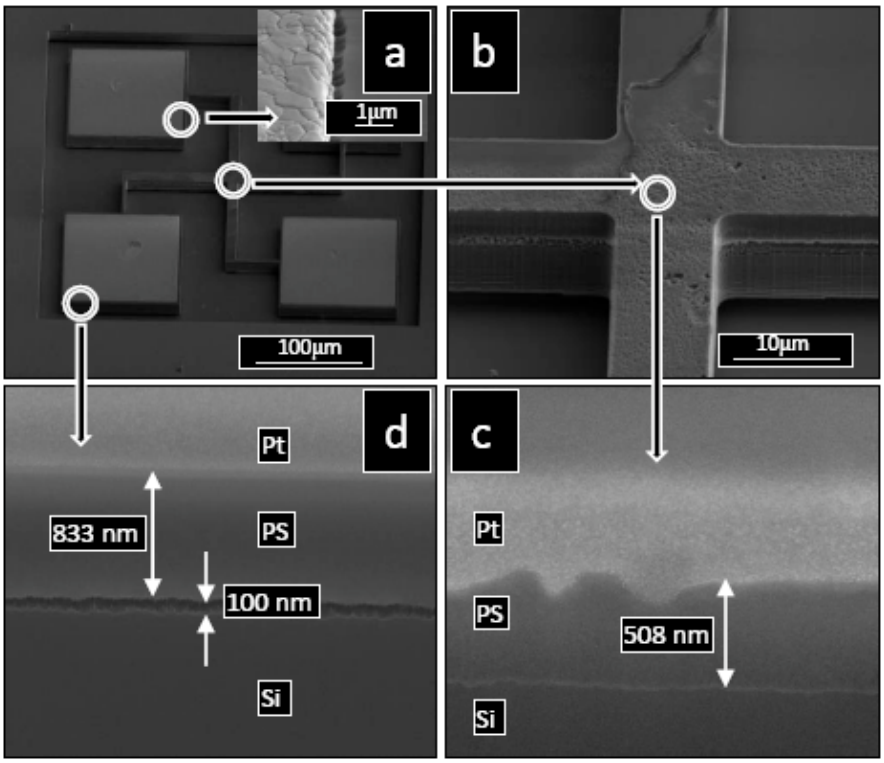

Figure 4: Four point probe structure after 24 minutes of immersion in (UDHF:H2O), including: (a) entire structure (oriented as in Fig. 1), (b) the gage section of the device - revealing "macroscopic" pitting and pores, (c) cross section of the gage region, and (d) the cross section of the region near the gold. . The inset of (a) shows the Au/Si interface on the probe structure. Bulk removal of Si is present and a trench several hundred nm in width has formed.

In order to compare the FEM results to empirical data, we exposed the four point probe polySi and SCS microdevices to the three electrolyte solutions, and subsequently analyzed the extent of galvanic corrosion using focused ion beam (FIB) milling of the structures. In short, the FIB cross-sections (an example is shown in Figure 4) importantly reveal that corrosion in microsystems structures is geometry dependent. The depth of porous silicon formed on the SOI resistive probe structures is expected to correspond with the magnitude of the current density on the SOI surface. Cross sections of the UDHF:H2O device indicate a gradient in depth that is greatest near the Au and a minimum in the gage section. A cross sectional trench along the entire length of one leed was made to specifically investigate the uniformity of the corrosion in areas of visual discoloration is shown in Figure 5. Large pits are seen at either end of the arm but in the middle the surface is relatively smooth. The thickness of the corroded layer varies by a factor of 6 (from 142 nm in the center to 852 nm near the Au) as indicated in the figure. Overall, the FIB cross-sectional data shows that a corrosion gradient is formed across the Si surface when exposed to UDHF and UDHF:H2O solutions, while the addition of the Triton surfactant to the to electrolyte solution yields uniform corrosion damage across the Si surface. In comparison, FEM results for the UDHF:H2O electrolyte are shown in Figure 6. Across the gauge section of the device, minimal gradient in potential/current is evidenced similar to simulation data for UDHF and UDHF:Triton.

The initial results of this study suggest that during the corrosion of actual resistive probe structures, the maximum current density induced by galvanic corrosion may be about an order of magnitude larger than originally thought. A

limiting factor in empirically determining the actual maximum corrosion current density on the device is ability to measure the thickness of the PS layer on the device upon a very brief, probably less than one minute, immersion. An additional discrepancy between the model and the empirical results hinges on the exact SAR of the as a result of stray sidewall etching of the device.

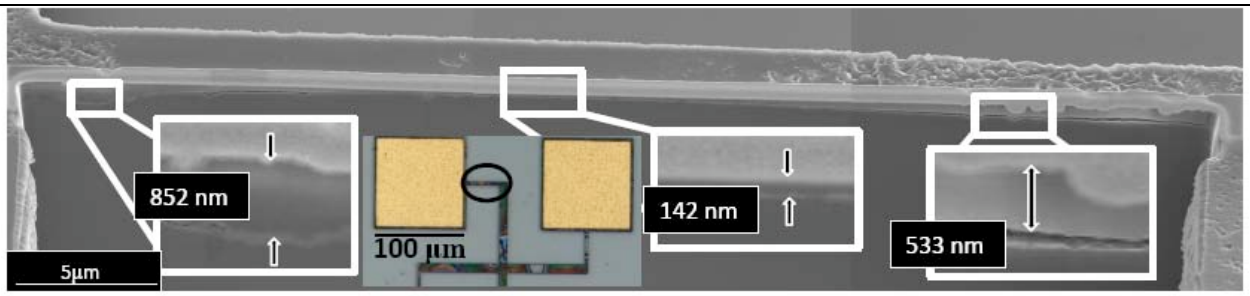

Figure 5: Thickness variation along a specific leed of the resistive probe structure, including comparison to visual appearance, obtained using FIB. The insets show the PS thickness along the arm. Also included is an optical image of the probe with the imaged arm circled.

Previous FEM analyses in the literature identifies corrosion behavior where the current density on the anode falls off as the distance from the cathode increases [9,10]. However, a model based on the actual micrometer dimensions of the device reveals a nearly uniform (within a few micro amperes (µA) per cm2) corrosion current density across the device. The UDHF:Triton device compares favorably to the FEM results in that it reveals a uniform optical coloration across the device and the FIB cross section clearly reveals a uniform etch depth. The UDHF:H2O device however shows broad discoloration and a definite etch gradient on the device. It is known that the UDHF:Triton electrolyte wets the Si surface much more effectively than the other two electrolyte compositions [3]. This enhanced wetting therefore allows the entire Si and Au areas to participate in the corrosion process whereas the UDHF:H2O electrolyte, by not wetting the full surface areas, does not allow the full electrochemical potential to develop across the structure. This phenomenon would not be taken into account in the FEM model, such that the model predicts a uniform current across the device and is unable to currently treat an inhomogeneous electrolyte/electrode interface.

In conclusion, this most recent ARO work demonstrates that a finite element simulation tool can be developed and applied to corrosion in Si Microsystems. Simple geometric test cases show that the finite element simulations accurately predict corrosion using the Tafel equation as a boundary condition. Electrochemical polarization curves of Si and Au in HF acid solutions are used for boundary conditions in a finite element model for four-point "Van der Pauw" resistive probe microscale devices. The modeling results are compared to the FIB cross sections of actual Si microdevices after exposure to HF acid solutions. The model reproduces the trend seen in empirical results for surface area ratio of Au to Si. Additionally, the model simulates a uniform corrosion current across the device as evidenced in actual Si Microsystems cross-sectioned by FIB milling.

Collaborative work with ARL

Starting in late 2008, my graduate student working on this ARO research project was awarded a SMART scholarship from the DoD. From this scholarship has resulted an ongoing research collaboration with researchers in the ARL Energetic MEMS group, with my student spending at least nine months per year working in their labs on PhD thesis research related to both the ARO and ARL efforts on galvanic porous Si formation, characterization, and optimization.

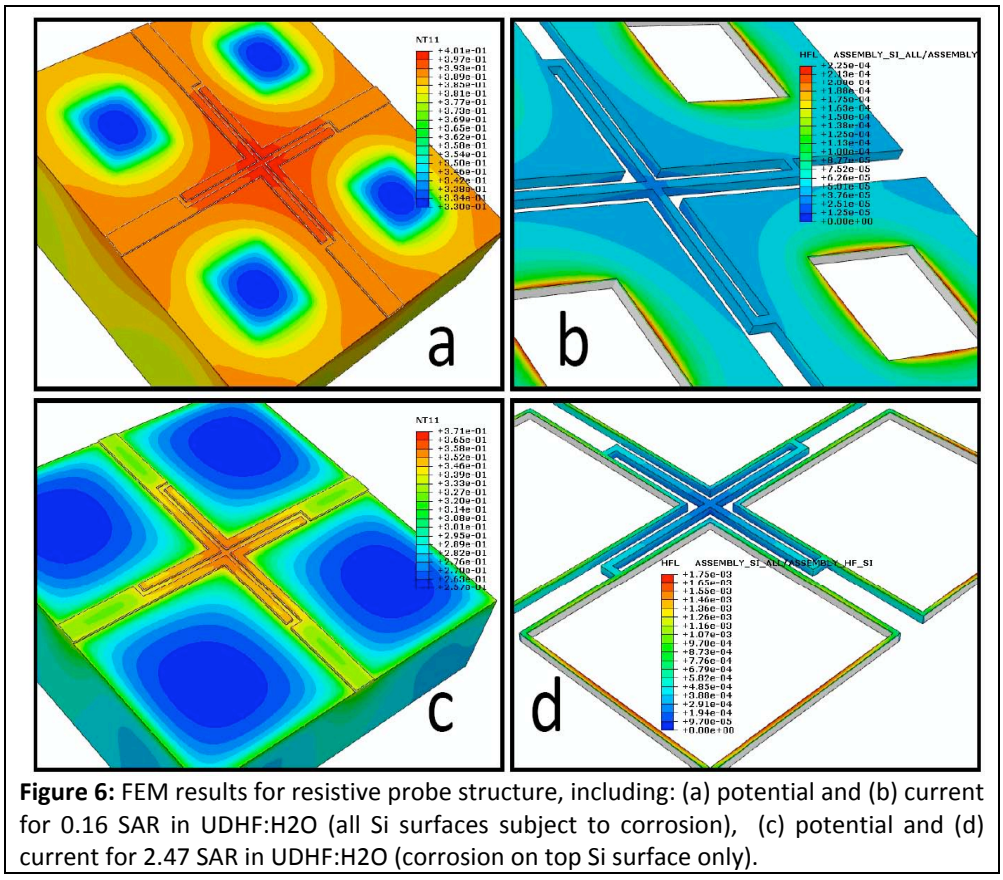

Figure 6: FEM results for resistive probe structure, including: (a) potential and (b) current for 0.16 SAR in UDHF:H2O (all Si surfaces subject to corrosion), (c) potential and (d) current for 2.47 SAR in UDHF:H2O (corrosion on top Si surface only).

[1] Miller, D.C., et al., Galvanic corrosion induced degredation of tensile properties in micromachined polycrystalline silicon. Applied Physics Letters, 2007. 90(19).

[2] Miller, D.C., et al., Connections between morphological and mechanical evolution during galvanic corrosion of micromachined polycrystalline and monocrystalline silicon. Journal of Applied Physics, 2008. 103(12).

[3] Miller, D.C., C.R. Becker, and C.R. Stoldt, Relation Between Morphology, Etch Rate, Surface Wetting, and Electrochemical Characteristics for Micromachined Silicon Subject to Galvanic Corrosion. Journal of the Electrochemical Society, 2008. 155(12): p. F253-F265.

[4] Redaelli, E., et al., FEM-models for the propagation period of chloride induced reinforcement corrosion. Materials and Corrosion-Werkstoffe Und Korrosion, 2006. 57(8): p. 628-635.

[5] Herbstritt, D., A. Weber, and E. Ivers-Tiffee, Modelling and DC-polarisation of a three dimensional electrode/electrolyte interface. Journal of the European Ceramic Society, 2001. 21(10-11): p. 1813-1816.

[6] Vankeerberghen, M., S. Gavrilov, and G. Nelissen, Finite element calculation of the polarisation behaviour of a metal in an aqueous solution using the dilute solution model. Corrosion Science, 2001. 43(1): p. 37-51.

[7] Lindeman, D., Steady-state current conduction analysis featuring electrochemical kinetics. Finite Elements in Analysis and Design, 1996. 22(3): p. 187-194.

[8] Doig, P. and P.E.J. Flewitt, A Finite-Difference Numerical-Analysis of Galvanic Corrosion for Semi-Infinite Linear Coplanar Electrodes. Journal of the Electrochemical Society, 1979. 126(12): p. 2057-2063.

[9] Jia, J.X., et al., Evaluation of the BEASY program using linear and piecewise linear approaches for the boundary conditions. Materials and Corrosion-Werkstoffe Und Korrosion, 2004. 55(11): p. 845-852.

[10] Jia, J.X., G.L. Song, and A. Atrens, Influence of geometry on galvanic corrosion of AZ91D coupled to steel. Corrosion Science, 2006. 48(8): p. 2133-2153.